Asymmetric optical microstructures driven by geometry-guided resist reflow

Jae-Jun Kim, Sung-Pyo Yang, Dongmin Keum, and Ki-Hun Jeong*

Department of Bio and Brain Engineering, KAIST Institute for Optical Science and Technology, Korea Advanced Institute of Science and Technology (KAIST), 291 Daehak-ro, Yuseong-gu, Daejeon, 305-701, South Korea
kjeong@kaist.ac.kr

Abstract: We report a new method, termed geometry-guided resist reflow, for the batch fabrication of asymmetric optical microstructures. Thermoplastic microstructures reflow along the geometric boundaries of the adjacent thermoset microstructures above the glass transition temperature of thermoplastic resin. The shape profiles can be freely formed as a concave, convex, or linear shape and the slope angle can also be tuned from 7 to 68 degrees, depending on the geometric parameters. This new method provides a new route for developing functional optical elements.

OCIS codes: (050.1950) Diffraction gratings; (050.6875) Three-dimensional fabrication; (220.4000) Microstructure fabrication; (230.3990) Micro-optical devices.

References and links

1. L. Li and A. Y. Yi, "Development of a 3D artificial compound eye," Opt. Express **18**(17), 18125–18137 (2010).
2. H. Yoon, S. G. Oh, D. S. Kang, J. M. Park, S. J. Choi, K. Y. Suh, K. Char, and H. H. Lee, "Arrays of *Lucius* microprisms for directional allocation of light and autostereoscopic three-dimensional displays," Nat Commun **2**, 455 (2011).
3. H. Xu, C. Yu, S. Wang, V. Malyarchuk, T. Xie, and J. A. Rogers, "Deformable, programmable, and shape-memorizing micro-optics," Adv. Funct. Mater. **23**(26), 3299–3306 (2013).
4. Y. P. Huang, H. P. Shieh, and S. T. Wu, "Applications of multidirectional asymmetrical microlens-array light-control films on reflective liquid-crystal displays for image quality enhancement," Appl. Opt. **43**(18), 3656–3663 (2004).
5. J. B. Kim, J. H. Lee, C. K. Moon, S. Y. Kim, and J. J. Kim, "Highly enhanced light extraction from surface plasmonic loss minimized organic light-emitting diodes," Adv. Mater. **25**(26), 3571–3577 (2013).
6. S. Möller and S. R. Forrest, "Improved light out-coupling in organic light emitting diodes employing ordered microlens arrays," J. Appl. Phys. **91**(5), 3324–3327 (2002).
7. M. K. Wei and I. L. Su, "Method to evaluate the enhancement of luminance efficiency in planar OLED light emitting devices for microlens array," Opt. Express **12**(23), 5777–5782 (2004).
8. S. Wooh, H. Yoon, J. H. Jung, Y. G. Lee, J. H. Koh, B. Lee, Y. S. Kang, and K. Char, "Efficient light harvesting with micropatterned 3D pyramidal photoanodes in dye-sensitized solar cells," Adv. Mater. **25**(22), 3111–3116 (2013).
9. L. Wang, X. Wang, W. Jiang, J. Choi, H. Bi, and R. Chen, "45° polymer-based total internal reflection coupling mirrors for fully embedded intraboard guided wave optical interconnects," Appl. Phys. Lett. **87**(14), 141110 (2005).
10. M. H. Nguyen, C. J. Chang, M. C. Lee, and F. G. Tseng, "SU8 3D prisms with ultra small inclined angle for low-insertion-loss fiber/waveguide interconnection," Opt. Express **19**(20), 18956–18964 (2011).
11. R. Voelkel, U. Vogler, A. Bich, P. Pernet, K. J. Weible, M. Hornung, R. Zoberbier, E. Cullmann, L. Stuerzebecher, T. Harzendorf, and U. D. Zeitner, "Advanced mask aligner lithography: new illumination system," Opt. Express **18**(20), 20968–20978 (2010).
12. D. Feng, G. Jin, Y. Yan, and S. Fan, "High quality light guide plates that can control the illumination angle based on microprism structures," Appl. Phys. Lett. **85**(24), 6016–6018 (2004).
13. J. H. Lee, H. S. Lee, B. K. Lee, W. S. Choi, H. Y. Choi, and J. B. Yoon, "Simple liquid crystal display backlight unit comprising only a single-sheet micropatterned polydimethylsiloxane (PDMS) light-guide plate," Opt. Lett. **32**(18), 2665–2667 (2007).
14. C. Waits, A. Modafe, and R. Ghodssi, "Investigation of gray-scale technology for large area 3D silicon MEMS structures," J. Micromech. Microeng. **13**(2), 170–177 (2003).
15. W. Yu, X. Yuan, N. Ngo, W. Que, W. C. Cheong, and V. Koudriachov, "Single-step fabrication of continuous surface relief micro-optical elements in hybrid sol-gel glass by laser direct writing," Opt. Express **10**(10), 443–448 (2002).
16. M. Han, W. Lee, S. K. Lee, and S. S. Lee, "3D microfabrication with inclined/rotated UV lithography," Sens. Actuators A Phys. **111**(1), 14–20 (2004).

#213725 - $15.00 USD Received 9 Jun 2014; revised 25 Aug 2014; accepted 26 Aug 2014; published 4 Sept 2014

17. A. Emadi, H. Wu, S. Grabarnik, G. D. Graaf, and R. F. Wolffenbuttel, "Vertically tapered layers for optical applications fabricated using resist reflow," J. Micromech. Microeng. **19**(7), 074014 (2009).
18. J. J. Kim, Y. Lee, H. G. Kim, K. J. Choi, H. S. Kweon, S. Park, and K. H. Jeong, "Biologically inspired LED lens from cuticular nanostructures of firefly lantern," Proc. Natl. Acad. Sci. U.S.A. **109**(46), 18674–18678 (2012).
19. H. T. Hsieh and G. D. J. Su, "A novel boundary-confined method for high numerical aperture microlens array fabrication," J. Micromech. Microeng. **20**(3), 035023 (2010).

1. Introduction

Surface relief microstructures enable highly efficient and ultrathin optical interfaces in imaging, display, lighting, light harvesting, or many other optical applications. They provide novel functions as well as serve as alternative substitutes with high performance. For example, microprisms on a curved surface, with optical asymmetry, or with shape memory polymers offer wide field-of-view imaging, auto-stereoscopic displays, or tunable optical film, respectively [1–3]. Besides, asymmetric microlenses enhance the brightness of reflective liquid-crystal displays [4], microcones or microlenses on organic light emitting diodes substantially improve light extraction efficiency [5–7], micropyramids on photoanodes increase the energy conversion efficiency of dye-sensitized solar cells [8], 45° micromirrors and microprisms provide high coupling efficiency of optical interconnection [9, 10], and microlens arrays optimize the irradiance uniformity of mask aligner illumination systems [11]. Moreover, micro-textured light-guide plate serves as a single optical sheet for ultrathin backlight unit rather than thick multiple sheets [12, 13]. These unique microstructures require asymmetric cross-sectional shapes with optical asymmetry such as triangle or saw tooth, which substantially increase their optical performance.

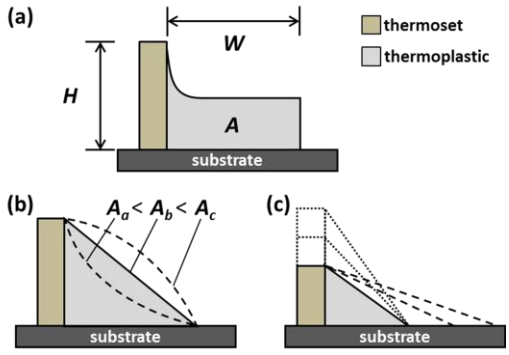

Fig. 1. Schematic illustration of geometry-guided resist reflow for the batch fabrication of surface relief microstructures with asymmetric profiles. (a) The reflow profile depends on the height of thermoset microstructures and the width and cross-sectional area of thermoplastic microstructures. (b) Thermoplastic microstructures thermally reflow along the geometric boundaries of thermoset microstructures. Depending on the cross-sectional area A of thermoplastic microstructures, thermoplastic microstructures adjacent to thermoset microstructures can be reformed into a linear ($A = A_b$), concave ($A_a = A < A_b$), or convex ($A_c = A > A_b$) shape in slope. (c) Control of the linear slope angles. The slope angle can be determined by a ratio of the height of a thermoset to the width of a thermoplastic microstructure.

For decades, the microfabrication methods of asymmetric microstructures have been extensively demonstrated by using gray-scale lithography [14], direct laser writing [15], inclined UV lithography [16], resist reflow [7], or wet-etching [8]. However, they still struggle in cost effectiveness or strict design rules for practical use; gray-scale lithography allows a large scale fabrication but still requires high cost for both equipment and photomask. Direct laser writing and inclined UV lithography are relatively low cost but not suitable for batch fabrication due to time-consuming fabrication or special configuration such as inclination and rotation stages, respectively. In addition, conventional resist reflow or wet-etching also allows a simple, low cost, and large area fabrication but still hampers the strict design rules for complex optical surfaces.

#213725 - $15.00 USD Received 9 Jun 2014; revised 25 Aug 2014; accepted 26 Aug 2014; published 4 Sept 2014

Here we report a simple and monolithic fabrication method for surface relief optical microstructures with asymmetric profiles by using geometry-guided resist reflow. Thermoplastic microstructures heated above the glass transition temperature (T_g) favorably reflow along the edge boundaries of adjacent thermoset microstructures (Fig. 1). The resultant reflow profile mainly depends on the height H of thermoset microstructures and the width W and cross-sectional area A of thermoplastic microstructures before resist reflow (Fig. 1(a)). Suppose the width and cross-sectional area of thermoplastic microstructures remain constant after resist reflow. The slope profile can be formed into a linear or curved shape depending on the cross-sectional area A due to the minimization of surface energy after resist reflow, where H and W are constant values (Fig. 1(b)). For instance, the slope curvature becomes either concave if the cross-sectional area is smaller than the triangular area of 1/2 H × W, i.e., A = A_a < 1/2 H × W or convex if A = A_c > 1/2 H × W. In particular, the linear slope can be achieved for A = A_b = 1/2 H × W. Consequently, the slope angle, i.e., $\tan^{-1}$ (H /W), can also be controlled by a ratio of the width of thermoplastic microstructures W to the height of thermoset microstructures H (Fig. 1(c)).

2. Batch microfabrication and optical characterization

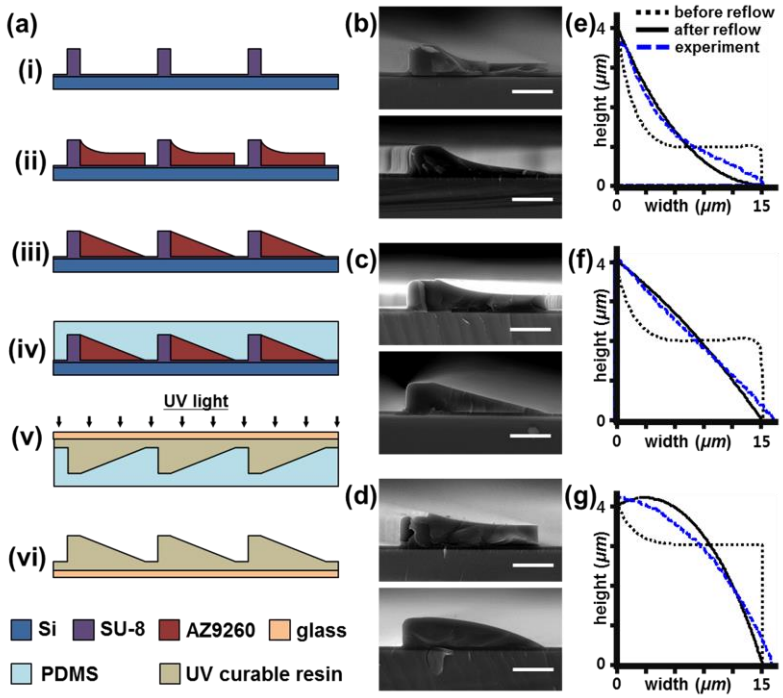

Fig. 2. (a) Monolithic fabrication method for asymmetric surface-relief microstructures. (i) photolithographic definition of thermoset (SU-8) resist, (ii) photolithographic definition of thermoplastic resist (AZ9260), (iii) thermal reflow above the glass transition temperature of thermoplastic resin, (iv) PDMS replication, (v) replica molding with UV curable optical resin, (vi) device relief from the PDMS replica. (b-d) SEM images of asymmetric microstructures before (top) and after (bottom) thermal reflow resulting in a (b) concave, (c) linear, and (d) convex shape in slope. Scale bar: 5 μm. (e-g) Comparison between the measured and calculated slope profiles of asymmetric microstructures after geometry-guided resist reflow (see also Media 1). Both the results clearly indicate the cross-sectional area of a thermoplastic microstructure determines the slope profile of asymmetric microstructure after thermal reflow.

Geometry-guided resist reflow has been experimentally demonstrated by using two-step photolithography, thermal reflow, and replica molding (Fig. 2(a)). Two-step photolithography was performed with a negative tone photoresist (SU-8, MicroChem) and a positive tone

#213725 - $15.00 USD Received 9 Jun 2014; revised 25 Aug 2014; accepted 26 Aug 2014; published 4 Sept 2014

photoresist (AZ9260, AZ Electronic Materials). The AZ9260 photoresist serves as a thermoplastic resin with T_g of 140 °C whereas the cross-linked SU-8 is a thermoset resin with high thermal stability [17]. First, thermoset resist was photolithographically defined on a 4 inch silicon wafer and thermoplastic resist was then defined on the predefined thermoset microstructures with precise alignment. Note that both microstructures were intentionally overlapped within the alignment tolerance in order to enfold the edges of thermoset microstructures with thermoplastic microstructures. Both the microstructures were thermally annealed at 180 °C for 1 hour on a hot plate in ambient conditions, where thermoplastic microstructures steadily reflow along the geometric boundaries of thermoset microstructures with thermal stability. All the microstructures were formed in a stable manner after surface energy minimization. Thin anti-stiction film of plasma-assisted fluorocarbon was then deposited on both the microstructures to facilitate polydimethylsiloxane (PDMS) replication [18]. The microstructures were finally transferred onto a UV curable optical resin (Norland optical adhesive 63) on a glass substrate after the PDMS replica molding.

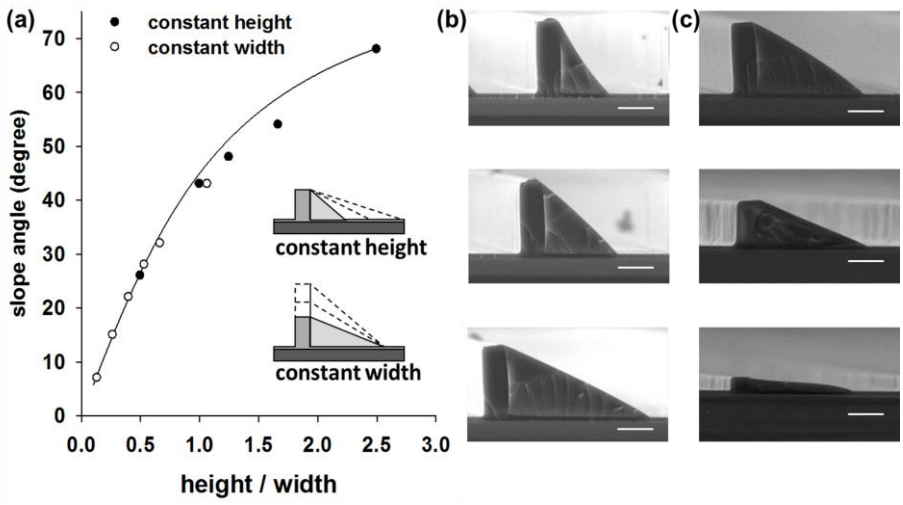

Fig. 3. The slope angles of asymmetric microstructures with a linear profile. (a) Change in the slope angles from 7 to 68 degrees depending on a ratio of the height of thermoset to the width of thermoplastic microstructures. The ratio can be precisely tuned by changing either the width of thermoplastic microstructures or the height of thermoset microstructures. The slope angle changes either from 68 to 26 degrees by changing the width of thermoplastic microstructures from 4 to 20 μm under a constant height of thermoset microstructures or from 7 to 43 degrees by changing the height of thermoset microstructures from 2 to 16 μm under a constant width of thermoplastic microstructures. Both the experimental results (constant height and width) are well fit to the solid line represents $\theta = \tan^{-1}(H / W)$, where θ is the inclined angle, H is the height of thermoset microstructures, and W is the width of thermoplastic microstructures. SEM images of asymmetric structures with (b) different widths of 6 μm, 10 μm, and 20 μm under a constant height of thermoset microstructures and (c) different heights of 2 μm, 6 μm, and 10 μm under a constant width of thermoplastic microstructures. Scale bar: 5 μm.

The experimental results clearly demonstrate that the cross-sectional area of thermoplastic microstructures substantially determines the slope profile of asymmetric microstructures. In experiment, the cross-sectional area of thermoplastic microstructures before reflow can be determined by considering the shrinkage of thermoplastic microstructures by vaporization of the solvent [19]. Figure 2(b)-2(d) shows the concave, linear, and convex profiles depending on the cross-sectional area of thermoplastic microstructures under a constant height of thermoset microstructures. In this experiment, the cross-sectional area of thermoplastic microstructures with linear profile was A = 30 μm^2 for H = 4 μm and W = 15 μm. The concave and convex profiles were also achieved for A < 30 μm^2 and A > 30 μm^2, respectively. The slope profiles were also numerically calculated by using a finite element method (COMSOL Multiphysics) (Fig. 2(e)-2(g)). Both the measured and calculated results

#213725 - $15.00 USD Received 9 Jun 2014; revised 25 Aug 2014; accepted 26 Aug 2014; published 4 Sept 2014

clearly indicate that the slope profiles of asymmetric microstructures depend on the cross-sectional area of thermoplastic microstructures.

The slope angle of asymmetric microstructures can also be precisely controlled by changing either the width of thermoplastic microstructures or the height of thermoset microstructures (Fig. 3). In experiment, the slope angle varies from 7 to 43 degrees for different thermoset height from 2 to 16 μm under a constant 15 μm width of thermoplastic microstructures and also from 68 to 26 degrees for different thermoplastic width from 4 to 20 μm under a constant 10 μm height of thermoset microstructures, respectively. The experimental results successfully demonstrate a precise and large tuning range of the slope angles from 7 to 68 degrees by changing a ratio of the width of thermoplastic microstructures W to the height of thermoset microstructures H (Fig. 3(a)). Figure 3(b) shows the SEM images of asymmetric optical microstructures with different widths for 6, 10, and 20 μm under a constant height of 10 μm and Fig. 3(c) shows with different heights for 2, 6, and 10 μm under a constant width of 15 μm.

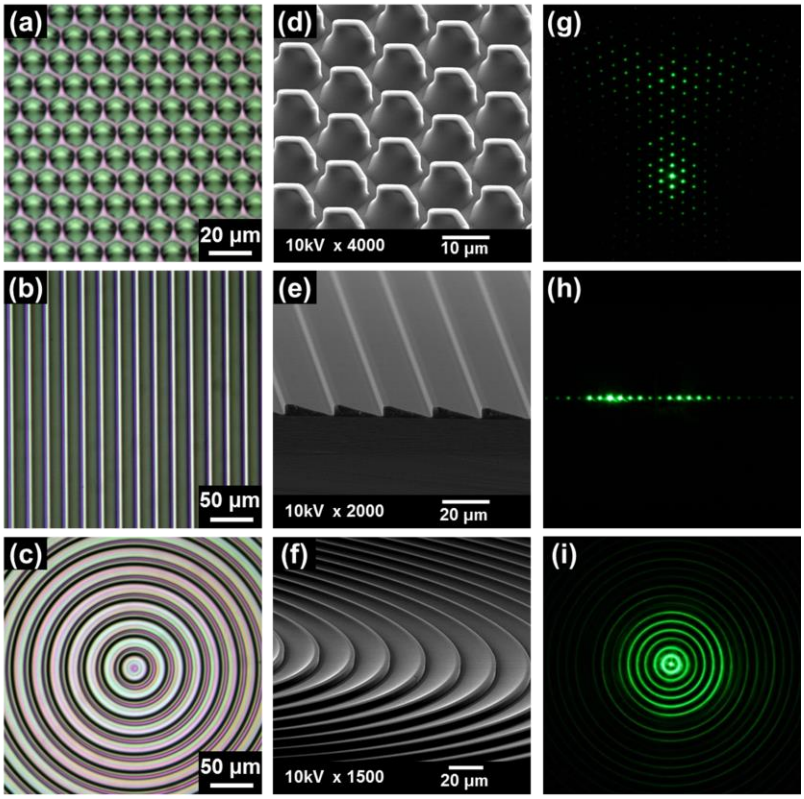

Fig. 4. (a-c) Optical and (d-f) SEM images of diverse surface relief optical microstructures with asymmetric profiles and (g-i) their light distributions at 532nm wavelength. Transmission hexagonal, line, and concentric ring elements with asymmetric profiles effectively modulate their light patterns by both diffraction and refraction.

Diverse optical microstructures with asymmetric profiles were further fabricated by using geometry-guided resist reflow (Fig. 4). Figure 4(a)-4(c) and 4(d)-4(f) show the optical and the perspective SEM images for hexagonal, line, and ring arrays with asymmetric microstructures, respectively. The interstitial gap between asymmetric microstructures was reduced up to 3 μm, i.e., the critical dimension for photolithography. Light distribution through the asymmetric microstructures was evaluated with a green laser (532 nm) line. Figure 4(g)-4(i) demonstrates the light distribution through their asymmetric periodic microstructures. Transmission hexagonal and line elements split incident light into two

#213725 - $15.00 USD Received 9 Jun 2014; revised 25 Aug 2014; accepted 26 Aug 2014; published 4 Sept 2014

different directions by both diffraction and refraction. In addition, concentric ring elements like a Fresnel lens with a negative slope efficiently distribute incident light into a radial direction. The experimental results clearly show that asymmetric optical microstructures effectively modulate light distribution by both diffraction and refraction.

3. Conclusion

To conclude, this work provides a new method for the facile and batch fabrication of surface relief optical microstructures with asymmetric profiles. Unlike conventional resist reflow methods, this geometry-guided resist reflow method can precisely control the slope profile of optical microstructures. Thermoplastic microstructures reflow along the geometric boundaries of the adjacent thermoset microstructures above the glass transition temperature of thermoplastic resin. The shape profile can be freely formed as a concave, convex, or linear shape depending on the cross-sectional area of thermoplastic microstructures. In particular, this method also enables the facile and batch fabrication of 3D optical microstructures with asymmetric or non-conventional shapes and thus provides a new route for developing functional optical elements such as diffractive optical elements (DOEs) with blazed angles, asymmetric microlenses, microprisms, or micromirrors. Furthermore, this method can also provide new opportunities for subwavelength optical structures such as diverse DOEs, plasmonic nanostructures, or meta-atoms with asymmetric profiles.

Acknowledgments

This work was supported by the National Research Foundation of Korea (NRF) grant (No. 2014022751, No. 2013050154), Center for Integrated Smart Sensors funded by the Ministry of Science, ICT & Future Planning as Global Frontier Project (CISS-2012M3A6A6054199), and Ministry of Trade, Industry, and Energy (MOTIE 10041120).